

Supplemental Information

Acetylation Dependent Compaction of the Histone H4 Tail Ensemble

*Sophia M. Dewing*¹, *Tien M. Phan*², *Emma J. Kraft*³, *Jeetain Mittal*^{2,4,5}, *Scott A. Showalter*^{1,3*}

¹Center for Eukaryotic Gene Regulation, Department of Biochemistry and Molecular Biology, The Pennsylvania State University, 77 Pollock Rd, University Park, PA 16802, USA

²Artie McFerrin Department of Chemical Engineering, Texas A&M University, 200 Jack E. Brown Engineering Building, College Station, TX 77843-3122, USA

³Department of Chemistry, The Pennsylvania State University, 376 Science Drive, University Park, PA 16802, USA

⁴Department of Chemistry, Texas A&M University, College Station, TX 77843, USA.

⁵Interdisciplinary Graduate Program in Genetics and Genomics, Texas A&M University, College Station, TX, 77843, USA.

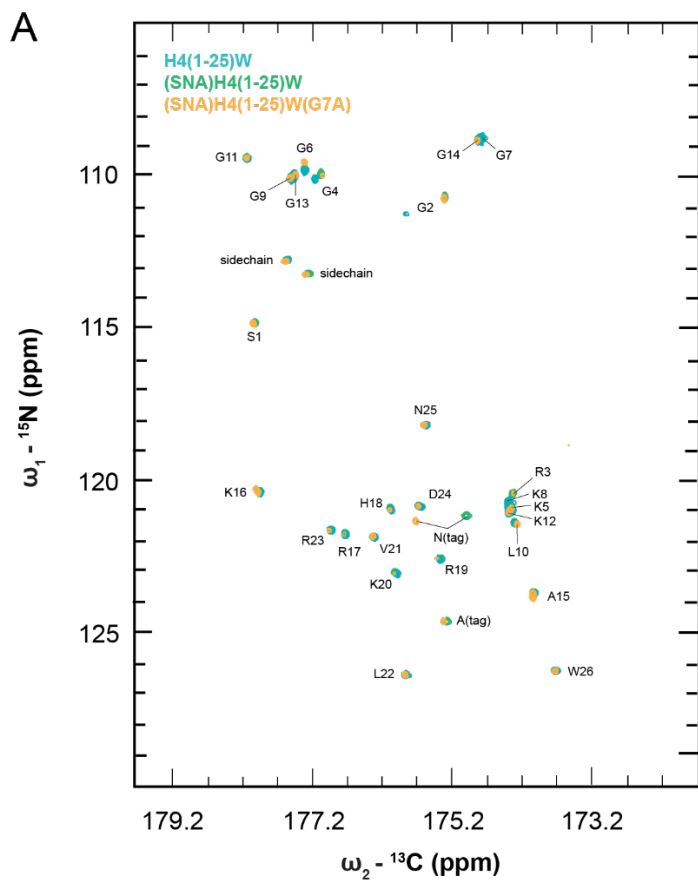


Figure S1. Overlaid ${}^{15}\text{N}$, ${}^{13}\text{C}$ -CON spectra used for assignments. Original chemical shift assignments were determined using (SNA)H4(1-25)W (green) and a G7A point mutant (yellow) to deconvolute chemical shift information in repetitive sequence regions. After assignments were complete, the cloning artifact (SNA) was removed for all downstream experiments. All spectra were recorded in 50 mM K_2HPO_4 , pH 7.2, 150 mM KCl.

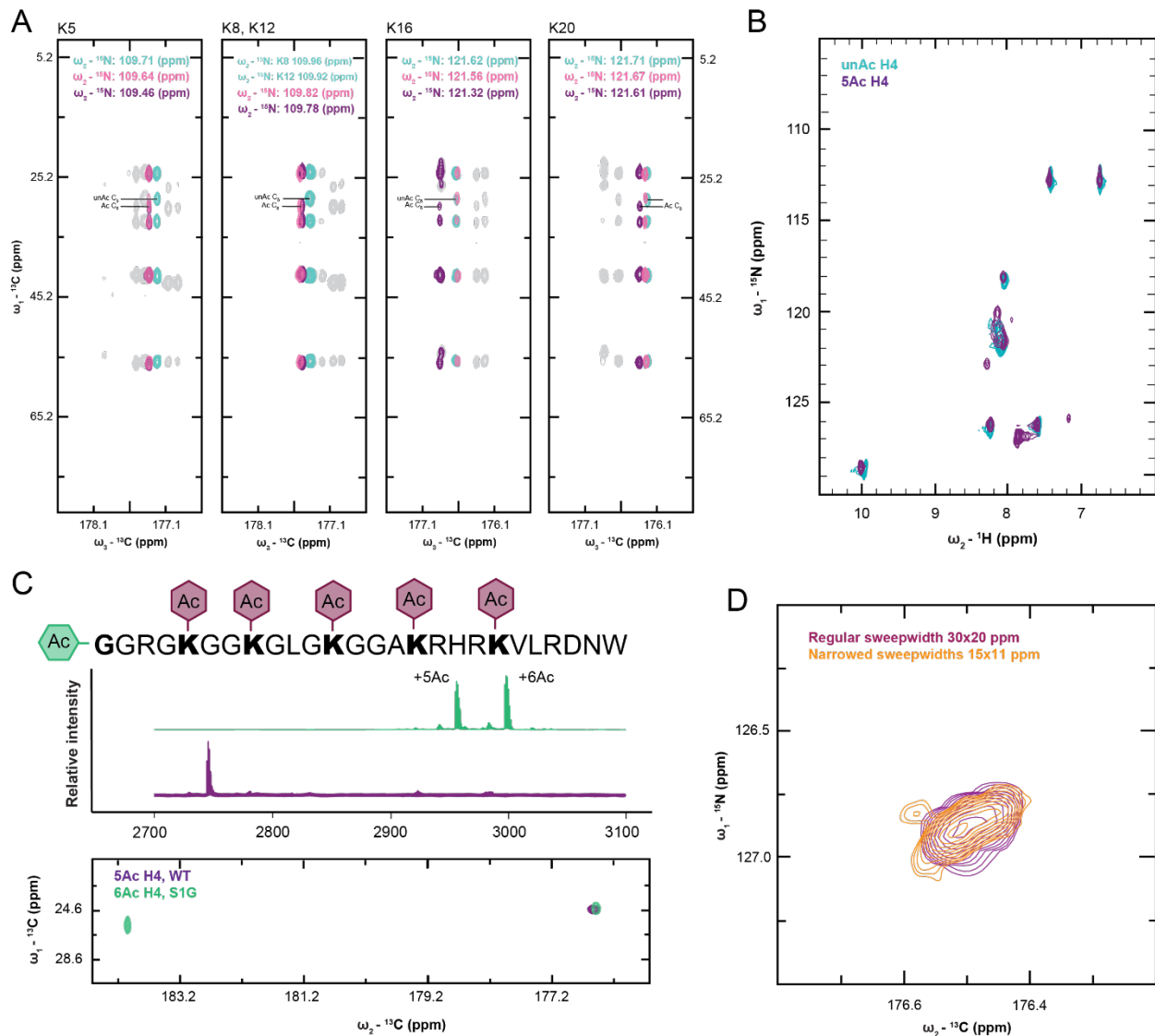


Figure S2. NMR and MALDI assignment of lysine acetylation. A) Overlaid ^{15}N , ^{13}C , ^{13}C -CCCON spectra for lysine residues K5, K8, K12, K16, and K20 in unAc (teal), 3Ac (pink), and 5Ac (purple) identifying which lysines are acetylated in each species. B) Overlaid ^{15}N , ^1H -HSQC spectra for unAc (teal) and 5Ac (purple) displaying poor spectral quality. C) Schematic of H4(S1G) acetylated at 5 lysine residues and the N-terminus (top); MALDI-MS spectra of 5Ac H4(WT) (purple) and 5/6Ac H4(S1G) (green) (middle); overlaid ^{13}C , ^{13}C -CaCO for 5Ac H4(WT) (purple) and 5/6Ac H4(S1G) (green) (bottom) showing the unique position of the N-terminal acetyl resonance. D) Zoomed overlay of ^{15}N , ^{13}C -CON spectra with typical (purple) or narrowed (gold) sweep widths demonstrating partially improved resonance dispersion. All NMR spectra were recorded in 50 mM K_2HPO_4 , pH 7.2, 150 mM KCl.

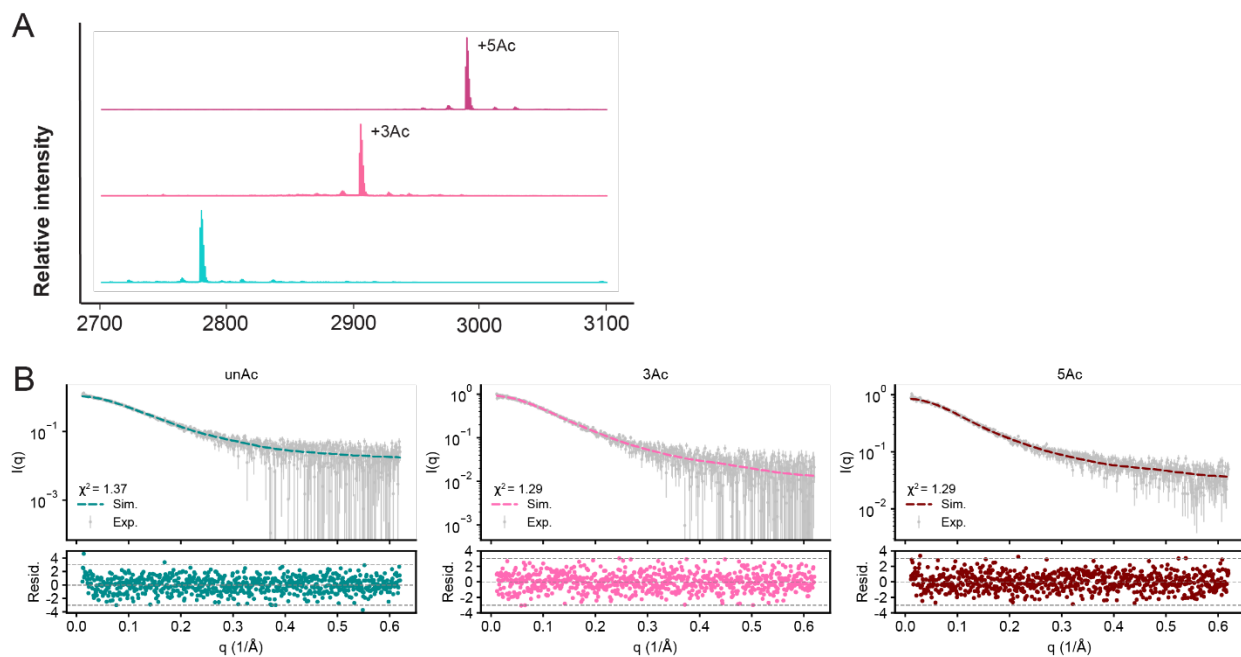


Figure S3. Small Angle X-ray Scattering data analysis. A) MALDI-MS quality control of unAc (teal), 3Ac (pink), and 5Ac (purple) Genscript synthesized H4 tail peptides used for SEC-MALS and SAXS. B) SAXS derived scattering profiles for unAc, 3Ac, and 5Ac (grey) compared to Crysol predictions show good agreement between experiment and theoretical methods.

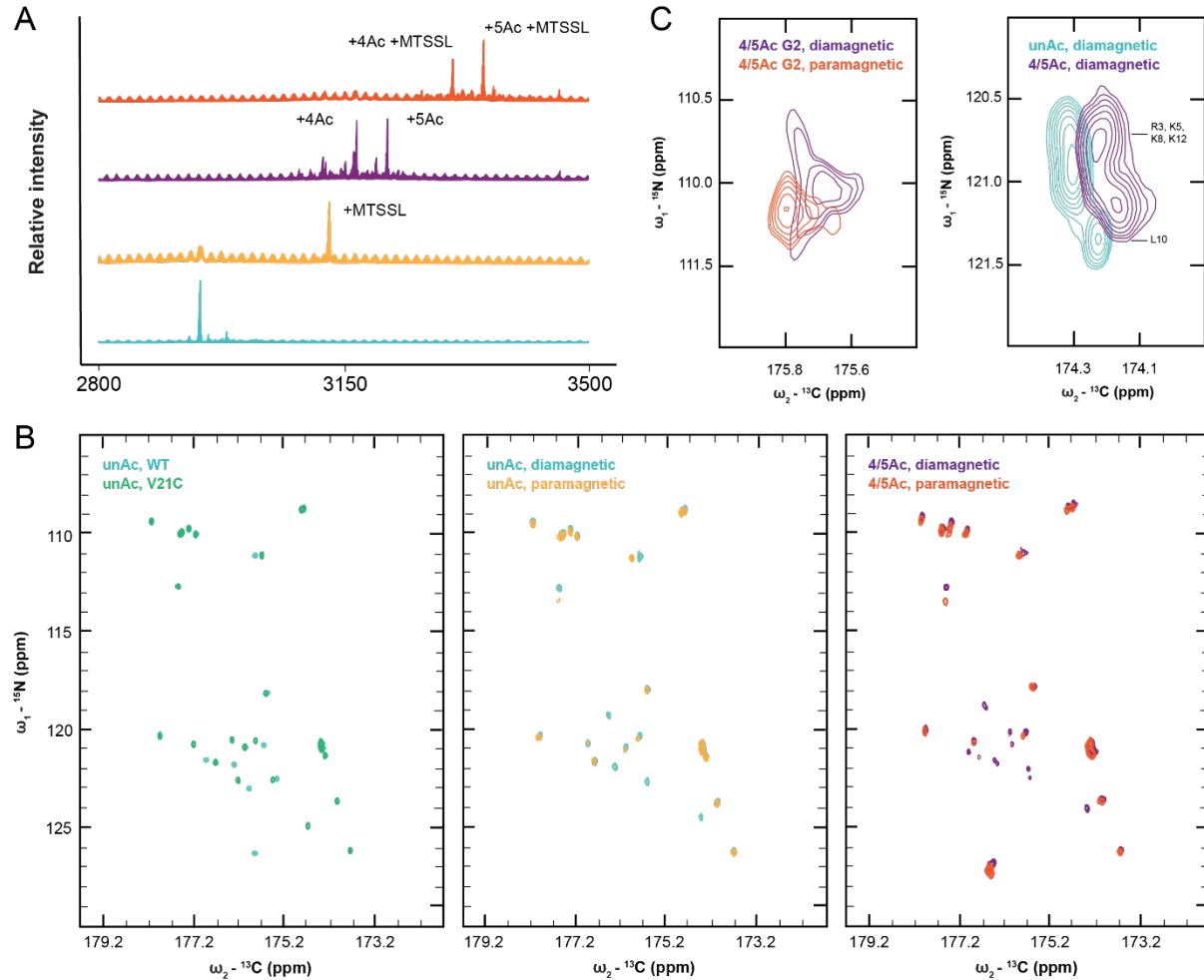


Figure S4. Spectra utilized for paramagnetic relaxation enhancement analysis. A) MALDI-MS spectra demonstrating MTSSL labeling efficiency for unAc (teal and gold) and 4/5Ac (purple and orange) samples. B) Overlaid ^{15}N , ^{13}C -CON spectra for unAc WT (teal) and V21C mutant (green) (left); unAc V21C conjugated with diamagnetic MTSSL (teal) and paramagnetic MTSSL (gold) (center); and 4/5Ac V21C conjugated with diamagnetic MTSSL (purple) and paramagnetic MTSSL (orange) (right). Note that the V21C mutant prevented complete acetylation, likely due to the proximity of K20. C) Zoomed ^{15}N , ^{13}C -CON spectra showing the unusual line shape of the G2 resonance for 4/5Ac V21C conjugated with diamagnetic MTSSL (purple) and paramagnetic MTSSL (orange) (left); degenerate resonances for R3, K5, K8, and K12 for unAc V21C conjugated with diamagnetic MTSSL (teal) and 4/5Ac V21C conjugated with diamagnetic MTSSL (purple) (right). All NMR spectra were recorded in 50 mM K_2HPO_4 , pH 7.2, 150 mM KCl.

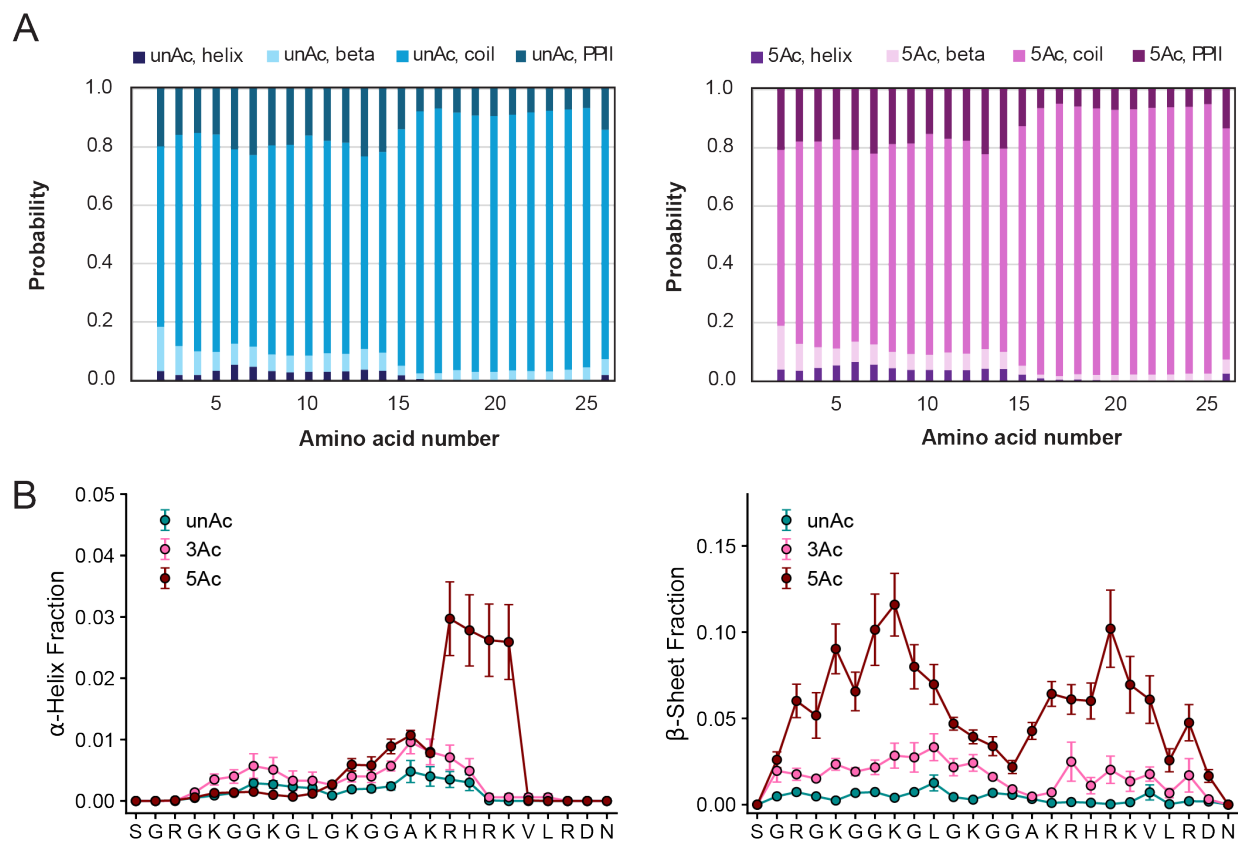


Figure S5. Secondary structure prediction from NMR and MD data. A) Raw probability outputs from $\Delta 2D$ webtool of secondary structure features for unAc (left, teal) or 5Ac (right, purple). B) Per-residue helix (left) and beta (right) fractions from simulations of unAc (teal), 3Ac (pink), and 5Ac (purple).

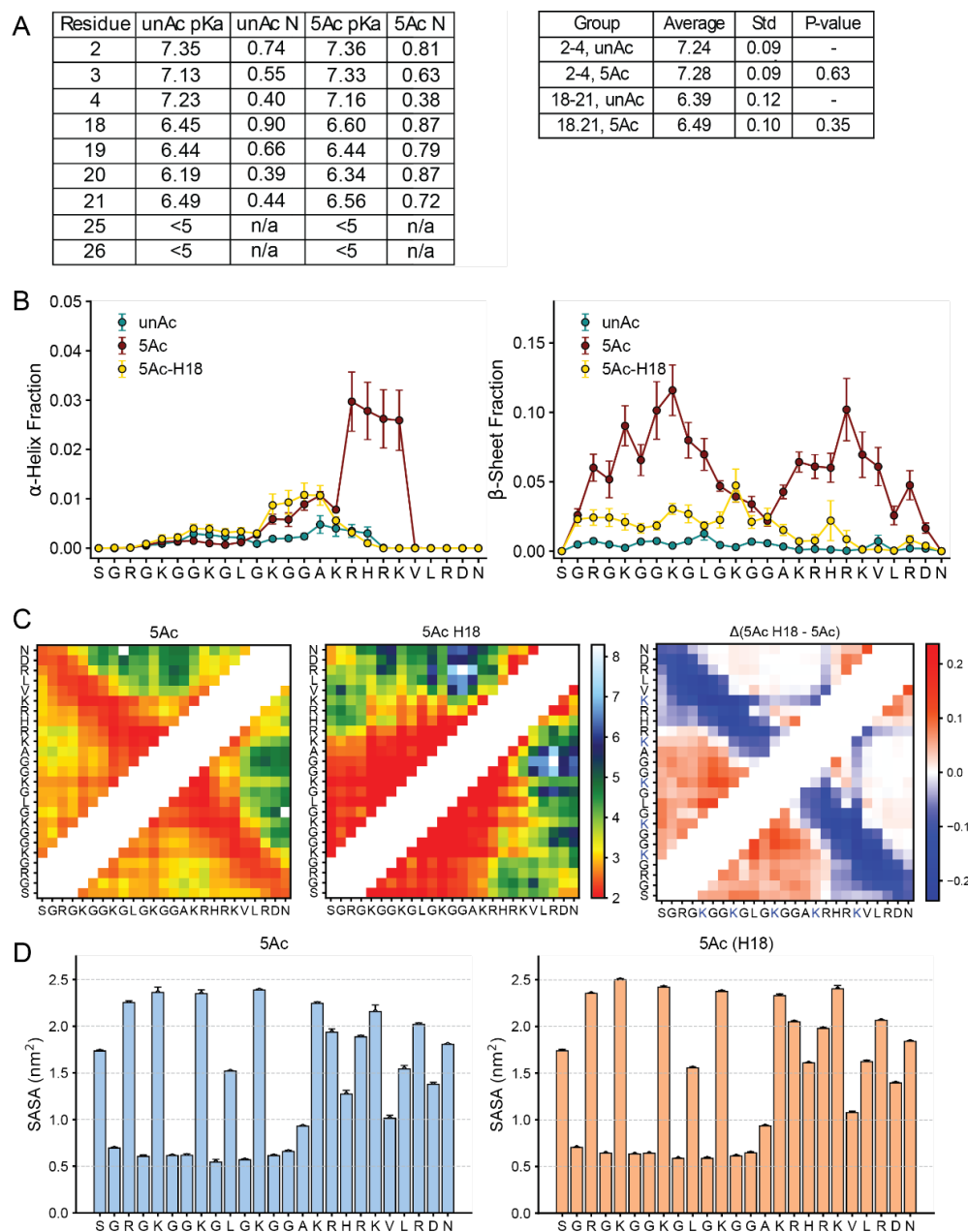


Figure S6. Changes in H4 tail physical properties as a function of lysine acetylation. A) Table of fitted pKa values and Hill coefficients (N) for individual residues (left) or collections grouped as reporters of each titration event (right). P-values were derived from Student's t-tests and relate to the significance associated with the difference in average pKa reported for each group of pKa values (residues 2-4 or residues 18-21). B) Per-residue helix (left) and beta (right) fractions from simulations of unAc (teal), 5Ac with H18 deprotonated (purple), and 5Ac with H18 protonated (gold). C) Intramolecular contact maps for 5Ac with H18 deprotonated (left), 5Ac with H18 protonated (center), or the difference between the two (right). D) Raw SASA for 5Ac with H18 deprotonated (left, blue) or 5Ac with H18 protonated (right, orange).

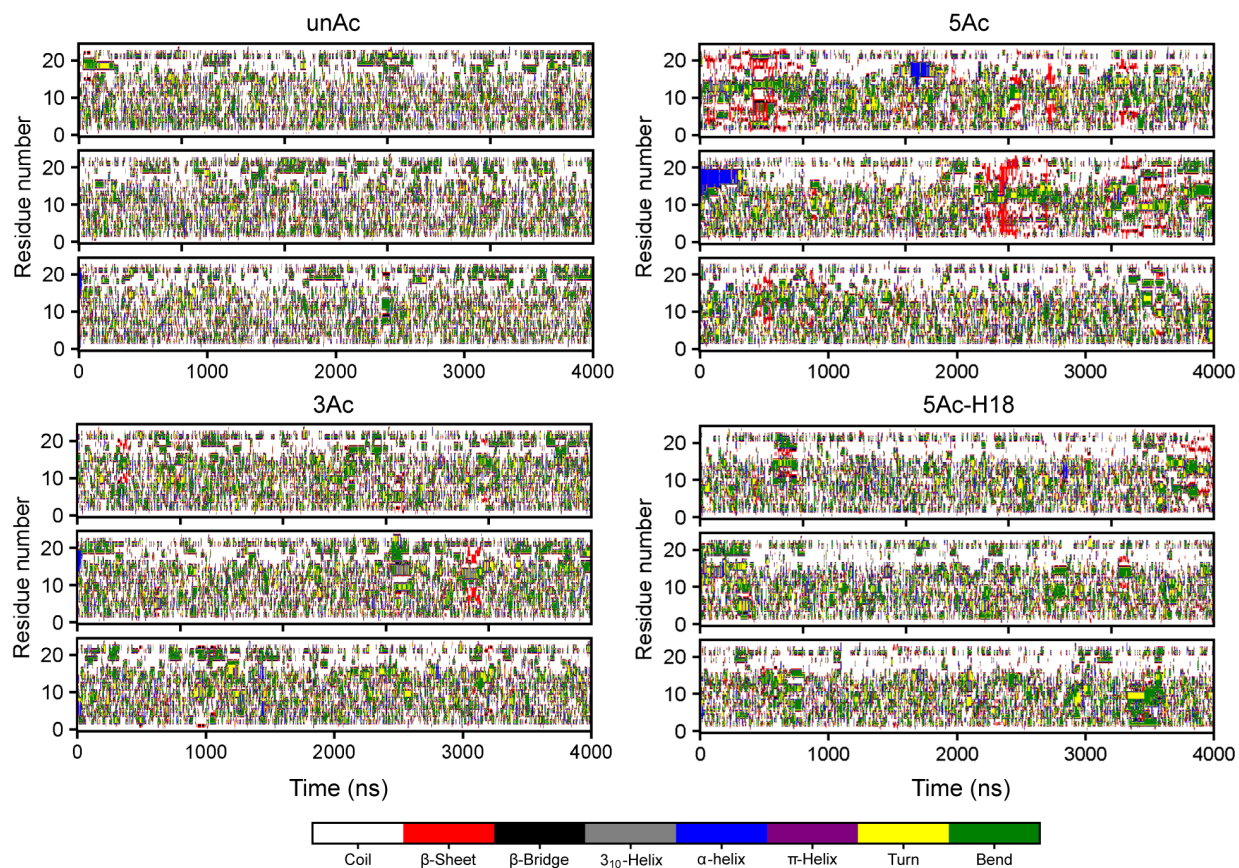


Figure S7. Secondary structure as a function of time in each of the twelve molecular dynamics simulations contributing to this work. For this study, the un-acetylated H4 tail, 3-acetyl H4 tail, 5-acetyl H4 tail, and 5-acetyl H4-tail were each subjected to three independent 4,000 ns simulations (3x4,000 ns). Secondary structure annotations are coded through the DSSP assignment of coil (white), β -sheet (red), β -bridge (black), 3_{10} -helix (grey), α -helix (blue), π -helix (purple), turn (yellow), or bend (green).